

# Design, Fabrication, and Testing of an Undergraduate Hall Effect Thruster

Braden Oh<sup>1\*</sup>, Albert Countryman<sup>2</sup>, Mahderekal Regassa<sup>3</sup>, Avery Clowes<sup>1</sup>, Grant Miner<sup>1</sup>, Simon Kemp<sup>1</sup>, S.C. “Mack” McAneney<sup>1</sup>, Marissa Klein<sup>3</sup> and Christopher Lee<sup>1</sup>

<sup>1</sup>Olin College of Engineering, 1000 Olin Way, Needham, 02492, MA, USA.

<sup>2</sup>Brandeis University, 415 South St, Waltham, 02453, MA, USA.

<sup>3</sup>Wellesley College, 106 Central St, Wellesley, 02481, MA, USA.

\*Corresponding author(s). E-mail(s): [boh@olin.edu](mailto:boh@olin.edu);

## Abstract

A multi-institutional team of undergraduate students conducted an independent study in which they designed, fabricated, and tested a small Hall effect thruster. The study was motivated by student desire to engage in a hands-on, multidisciplinary project in the field of space propulsion. This paper represents the outcome of this educational experiment. It describes the educational framework followed; the fundamental physics behind Hall thruster operation (at an early undergraduate level); the design process followed to develop and construct the thruster including a novel additively-manufactured propellant diffuser; and testing results. The thruster did not successfully ignite during testing. The cathode/plasma source was identified as the likely point of failure; rather than design flaws in the thruster itself, thereby introducing next steps for a future study following a similar framework. The educational program presented serves as a case study for a small-team undergraduate space propulsion project with limited resources and prior knowledge as well as a technical reference and knowledge base for future teams attempting a project of similar scope.

**Keywords:** Hall thruster, Undergraduate, Fundamentals, Education

# 1 Introduction

Electric propulsion engines operate on the principle of generating and expelling ions at very high speeds. In a Hall effect thruster (HET), a plasma is formed within an annular channel and an axial electric field is used to accelerate and eject plasma ions to generate thrust. The plasma is generally formed by bombarding a gaseous propellant, such as xenon or krypton, with high energy electrons trapped by a radial magnetic field. The radial magnetic and axial electric fields allow trapped electrons at any location within the annular channel to "drift" in the direction perpendicular to both fields, giving rise to an azimuthal, drift-enabled Hall current that gives the HET its name.

Seeking to understand these concepts for the first time, nine undergraduate students from three colleges (five sophomores, two juniors, and one senior) majoring in a variety of engineering and physics disciplines designed, fabricated, and tested a 50mm, 300W HET during the 2021-22 academic year. This project was driven by students' internal motivations to learn electric propulsion concepts and was undertaken for credit through Olin College of Engineering's independent study framework.

This paper represents the outcome of this student-led, undergraduate learning experience. It aims to guide future teams of undergraduate students by communicating the structure of the educational program followed (section 2); detailing the physics principles that drive HET design (sections 3.1-3.2); walking through the process used to design this HET (sections 3.3-3.6); presenting a low-cost thrust stand design (section 4); and communicating the ignition test results and next steps for the project (section 5). In this manner, the educational project presented may serve as a case study and a technical reference for future teams attempting a project of similar scope.

# 2 Educational Program

The development of Hall thrusters has been the subject of a senior-level, undergraduate thesis [1] and graduate-level research [2] but is rarely, if ever, a component of the initial portion of an undergraduate curriculum. In 2020, a previous team of Olin College students demonstrated that the self-directed development of a HET is a feasible undertaking for students who have completed only one year of undergraduate studies [3]. Using the independent-study curriculum of the previous team as a model, students at Olin and Wellesley Colleges and Brandeis University engaged in a new self-directed study motivated by the students' internal desire to learn key concepts behind electric propulsion and to engage in a hands-on and multidisciplinary engineering development project. In addition, this study introduced undergraduate students to the research process and provided opportunities to develop written and oral technical communication and proposal writing skills.

## 2.1 Multi-institutional Program Organization

The project was scoped as a pair of single-semester (14 week) independent studies sponsored by Olin College, allowing students to receive course credit, software access, and faculty advisement from Olin (although no funding was received in this manner). Each independent study required a proposal that outlined course curriculum, timelines, deliverables, and grading schema, authored by the student team and signed off by a faculty advisor (copies of the proposals may be obtained from the lead author). Students with different academic backgrounds enrolled in the study together; an open cross-enrollment consortium exists between Wellesley, Brandeis, and Olin, enabling students from all three schools to participate for credit.

Olin features a project-based engineering curriculum, but does not have a physics department. By contrast, Wellesley and Brandeis feature physics programs, but lack engineering opportunities. Uniting students from all three schools, the team included astrophysics, physics, mechanical engineering, and electrical engineering majors. These cross-cutting backgrounds allowed individual team members to deepen individual knowledge through both teaching and learning from each other. All team members and their host schools' aerospace communities benefited from relationships built with industry and academic experts.

## 2.2 Project Scope and Aims

Key activities of the first semester included performing a literature review, designing and computationally modeling the electromagnetic fields in a HET, participating in a design review, and securing necessary funding. The second semester focused on manufacturing, assembling, and testing the thruster. In both semesters the activities were entirely student-led except for a weekly or bi-weekly check-in with the advising professor. The study as a whole had three major goals:

1. Create a hands-on, collaborative experience for students across institutions and disciplines
2. Learn the principles behind, design, and test a Hall effect thruster
3. Simulate the research environment through grant writing and technical communication.

The first goal was achieved through the multi-institutional program as previously discussed. The second goal was achieved by studying a variety of published textbooks, technical papers, and graduate theses, including [1, 3–9]. As difficulties and gaps in understanding were encountered, the team directly contacted corresponding authors and experts in the field.

Graded deliverables included meeting minutes, detailed literature review notes, written grant proposals, a COMSOL Multiphysics magnetic field model, final CAD models, and manufactured thruster hardware. Examples of hardware deliverables include electromagnets and magnetic shunt, thruster

#### 4 *Undergraduate Hall Thruster*

channel, gas feed pipes, propellant diffuser, and hot cathodes. An additional goal, which was added partway through the second semester, was to design and fabricate a test stand capable of measuring forces on the order of tens of millinewtons. Testing took place in the MIT Space Propulsion Laboratory's AstroVac chamber, with time and laboratory resources donated by Professor Paulo Lozano.

The third goal was met by engaging in a variety of activities typical to the research process. First, a formal literature review was conducted; this was the first literature review that several students had participated in, introducing them to the crucial skill of studying and documenting prior literature. Second, Olin College does not provide funding for independent studies, so alternative means of funding were secured through student grants. Separate proposals were written and filed to secure a Babson-Olin-Wellesley (BOW) Three-College Collaboration Presidential Innovation Grant and an Olin College Student Academic Grant (SAG), both of which were successfully won. This was the first exposure to grant proposal writing for all students on the team. Third, a design review was conducted, requiring students to communicate design decisions in both a written and oral manner to experts from industry and academia. Fourth, an abstract was submitted to the International Electric Propulsion Conference (IEPC). This was the first abstract that several students had co-authored. Finally, the team pursued a patent for their gas diffuser; on May 11, 2022 the team filed US provisional patent application no. 63/340566 for an additively manufactured azimuthal gas diffuser.

### **2.3 Project-Based Undergraduate Curricula**

Olin's pedagogical approach of project-based learning, in tandem with giving students greater control over the design of their courses of study, has proven to be valuable across many aspects of engineering education [10]. An added benefit of this setting is that students of different backgrounds often teach each other, serving to both reinforce existing skills and strengthen personal technical communication skills.

At the start of the project, the team collectively had knowledge spanning electromagnetism, particle and plasma physics, thermodynamics and statistical mechanics, and material, electrical, mechanical, and computer engineering, though no single student was versed in all fields. Because HET design requires considerations that span all of these fields, students were required to gain cross-cutting expertise in order to experience success: engineering students engaged in science topics such as electricity and magnetism, particle and plasma physics, and materials science. Meanwhile, physics students practiced applied engineering skills such as modeling and simulation, instrumentation, design for manufacturing, and fabrication. Across majors, students were able to both strengthen and develop new skills and core competencies

This project's unique format of a student-led, multi-disciplinary technical development project allowed skills critical to the research process to be developed in a more engaging (and therefore more impactful [11]) manner than in a traditional classroom setting.

## 3 Thruster and Cathode Design

The previous Olin College team developed a small, permanent-magnet HET which demonstrated an unstable pulsed fire with an argon propellant [3]. Correspondence with members of the previous team revealed four suggestions for major design revisions: increase the volume to surface area ratio of the thruster channel to reduce wall losses; use electromagnets to enable real-time magnetic field variation; use krypton, a more easily-ionizable propellant; and avoid using a hollow cathode, which is difficult to build and prohibitively expensive to purchase. These considerations were taken into account when designing this study's thruster, in tandem with fresh learning performed as a part of the independent study. The entire design process followed, from physics principles to design applications, is outlined in this section.

### 3.1 Starting-Point Parameters & Scaling Laws

The so-called “tyranny of the rocket equation” comes down to a problem of propellant weight: as propellant is added to a spacecraft, the system mass increases and an increasing long thruster burn becomes necessary to accelerate the greater system mass. This places a practical upper limit on the amount of fuel carried, as at a certain point only marginal changes in velocity ( $\Delta v$ ) can be achieved for the addition of more propellant. A thruster’s momentum transfer efficiency can be maximized by maximizing the exit velocity of propellant,  $v_{ex}$ ; this in turn reduces the amount of propellant necessary to attain a desired  $\Delta v$ . Electric propulsion engines accelerate propellant to much higher speeds than can be achieved by chemical rockets by means of electromagnetic fields, serving as a class of thrusters which generate lower levels of thrust than chemical rockets but with much higher propellant exit velocities (and hence a higher specific impulse). This team chose to undertake the design and construction of a Hall effect thruster.

Three parameters define the initial design constraints for a thruster: thrust, specific impulse, and power. Thrust,  $T$ , represents the amount of force that the device is capable of generating. Specific impulse,  $I_{sp}$ , represents the ratio between the thrust and the weight flow of propellant (the ratio between  $T$  and  $\dot{m}g$ , which is equivalently  $\dot{m}v_{ex}/(\dot{m}g)$ ) and represents the efficiency of a rocket to produce a net change in velocity. In this context, power represents the power of the anode-to-cathode circuit, in which electrons flow from the cathode to the anode through the plasma within the thruster channel. When designing a thruster, two of these quantities must be chosen by on the requirements/limitations of the mission or spacecraft design. The final quantity is then determined from the former two. The three defining parameters

## 6 Undergraduate Hall Thruster

are related to one another via ion mass flow rate,  $\dot{m}$ , and ion exhaust velocity,  $v_{ex}$ , in the following manner:

$$I_{sp} = \frac{v_{ex}}{g} \quad (1)$$

$$P = \frac{\dot{m}v_{ex}^2}{2\eta} \quad (2)$$

$$T = \dot{m}v_{ex}. \quad (3)$$

The authors note that the overall propellant mass flow rate to the thruster is comprised of both an ion flow rate (the ionized portion of the propellant) and a neutral flow rate (the unionized portion of the propellant, which contributes considerably less momentum to the spacecraft). If the ionization rate of the plasma can be estimated, the propellant mass flow rate may be adjusted to ensure a particular ion flow rate is achieved.

As estimating a realistic exhaust velocity can be difficult, the team instead started by examining the operating parameters of an SPT-100 Hall thruster [9] and applied a set of scaling laws reported by Goebel and Katz [4] to select relevant dimensions for the thruster. The authors note that more recent and advanced scaling laws have been derived since Goebel and Katz's 2008 publication, such as those published by Dannenmayer in 2011 [12] or Lee [13] in 2019. However, the authors found the Goebel and Katz publication more accessible given their absence of prior experience in the field, so this thruster was designed following the older set of scaling laws.

Two thrusters operating at a similar voltage will accelerate ions through a similar potential, thus resulting in similar exhaust velocities (neglecting design-specific losses) and therefore  $I_{sp}$ ; for this reason, the team decided to use the same operating voltage as the SPT-100 and accordingly assumed a similar  $I_{sp}$ . These scaling laws are

$$P \propto R^2 \quad (4)$$

$$T \propto R^2 \quad (5)$$

$$w \propto R \quad (6)$$

where  $R$  represents the outer radius of the thruster channel and  $w$  represents the width of the channel (the difference between the outer and inner radii).

The student team chose to design a half-scaled version of the SPT-100. Using an anode voltage of 300V, the scaling laws defined a channel with outer radius 25mm and width of 7.5mm, and predicted a power of 337.5W and a thrust of 21.7mN. Goebel and Katz's scaling laws do not take into account features of a thruster that could affect the scaled parameters (such as ionization efficiency or loss of energy to wall collisions). As a result, the student team performed an alternate set of calculations to verify the scaling law predictions. This was done using equations 1, 2, and 3 with the power predicted by equation 4 and assuming a thruster efficiency,  $\eta$ , of 0.4 and an  $I_{sp}$  of 1600,

which is the reported efficiency of the SPT-100 studied by Sankovic, Hamley, and Haag in 1994 [9]. This yields,

$$T = \frac{2\eta P}{I_{sp}g} = 17.2 \text{mN} \quad (7)$$

$$\dot{m} = \frac{T}{I_{sp}g} = 1.096 \frac{\text{mg}}{\text{s}}. \quad (8)$$

Given that 100% propellant ionization is impossible in practice, this value provides a lower bound to the mass flow rate used in experiments.

### 3.2 Electric and Magnetic Field Concepts

Propellant is ionized via bombardment from electrons trapped in the main channel. Electrons are trapped by a radial magnetic field. An axial electric field is then applied such that electrons experience  $\vec{E} \times \vec{B}$  drift, resulting in an azimuthal velocity (a drift-enabled Hall current). The purpose of the device's electric field is to both transport electrons from the cathode into the channel and to accelerate ionized propellant away from the thruster.

The cathode has a negative potential with respect to the anode so that electrons that are produced by the cathode are drawn into the channel. Given that the magnetic field is what traps electrons within the channel, they require a certain velocity to stay trapped. They remain for a time within the plasma in the channel, but eventually lose energy through collisions with the wall or other particles (such as neutrals). When an electron reaches the anode at the bottom of the channel it re-enters the circuit and is delivered back to the cathode.

It is notable that a Hall thruster plasma maintains quasineutrality; if the total charge of the plasma becomes biased in one direction or the other, the plasma will return to neutrality either by pulling back charges of the opposite sign or expelling charges of the same sign as the bias. A power supply connects the thruster anode to the cathode. This supply serves to move electrons captured on the thruster anode into the cathode, where they are expelled into the thruster's ion beam to neutralize the plume. If this were not the case, the spacecraft would build up a net negative charge as ions are ejected and emitted ions would be pulled back towards the thruster, returning any change in momentum gained by having fired them in the first place.

The principles of  $\vec{E} \times \vec{B}$  drift can be conceptualized as follows. Imagine a region of space with a uniform magnetic field. A charge moving in this field will travel in circles endlessly. Next, consider the same setup with a uniform electric field oriented perpendicularly to the magnetic field. When the charge is at a point of higher electric potential, it will possess less kinetic energy and will travel more slowly; conversely, at a point of lower electric potential, it will travel more quickly. This causes the particle to alternate between a tight orbit and a large orbit (in lower and higher potential regions, respectively) and results in a drift perpendicular to both the electric and magnetic field. A

8 *Undergraduate Hall Thruster*

sample trajectory of a particle trapped within such a field is shown in Fig. 1.

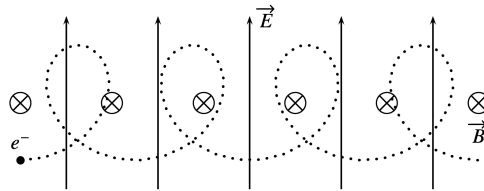


**Fig. 1:** The cycloidal trajectory of an electron undergoing  $\vec{E} \times \vec{B}$  drift in a uniform electric and magnetic field. The electron tends to circle counterclockwise in the magnetic field, but the electric field imposes an additional constant acceleration that causes it to travel faster at the bottom of the circle. The net result is a constant rightward drift velocity.

This phenomenon is known as  $\vec{E} \times \vec{B}$  drift and is the central mechanism that allows for electrons to be trapped within the thruster's channel in an azimuthal flow (this is the Hall current that gives Hall thrusters their characteristic name). To set up this azimuthal flow with an axial electric field, the magnetic field must be oriented radially. In order to best prevent electrons from escaping, the magnetic field is designed to be strongest at the exit plane of the thruster channel. A useful way to characterize the magnetic field in a thruster is by the gyroradii of the ions present in the system (this radius is referred to in the field as the Larmor radius). The Larmor radius for a generic charge in a magnetic field can be found as,

$$r_q = \frac{mv_\perp}{qB} \quad (9)$$

where  $r_q$  is the Larmor radius for a particle of mass  $m$  and charge  $q$ , with velocity perpendicular to the  $B$  field of magnitude  $v_\perp$ . Even in the presence of an electric field that causes charged particles to drift, those particles will still travel in circles that are roughly similar to their behavior in the absence of such a field, hence the Larmor radius can be calculated with knowledge of the magnetic field strength along with particle speed, mass, and charge. For particles in a Hall thruster, Goebel and Katz [4] report the Larmor radii to be,

$$r_e = \frac{1}{B} \sqrt{\frac{8m_e k T_e}{\pi e}} \quad (10)$$

$$r_i = \frac{1}{B} \sqrt{\frac{2m_i V_b}{e}} \quad (11)$$

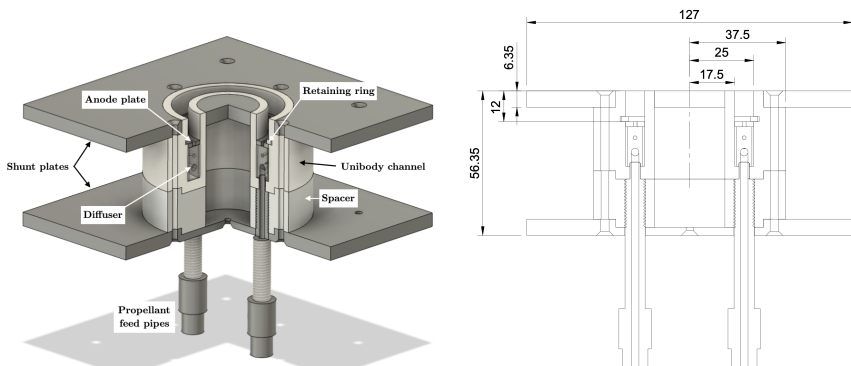
where  $r_e$  and  $r_i$  are the Larmor radii of an electron and ion, respectively;  $B$  is the radial magnetic field strength;  $m_e$  and  $m_i$  are the masses of an electron

and ion, respectively;  $T_e$  is the electron temperature<sup>1</sup> in units of eV;  $k$  is Boltzmann's constant;  $V_b$  is the thruster beam voltage; and  $e$  is the fundamental charge. In order to trap electrons without trapping ions, the channel length must be significantly longer than the electron Larmor radius and significantly shorter than the ion Larmor radius. This is generally easy to achieve because the differences in order of magnitude between the mass of an electron and an atom of propellant (on the order of  $10^6$ , depending on propellant used) gives rise to orders of magnitude difference between Larmor radii.

### 3.3 Designing the Magnetic Field

The team selected an anode voltage of 300V, yielding an approximate electron temperature of 30eV. The peak magnetic field strength (the field strength at the exit plane of the channel) was selected to be 30mT, which is on a similar order of magnitude to thrusters designed by Baird [1], Warner [7], and the prior Olin College team [3]. Krypton propellant was selected for being substantially cheaper than xenon while still having a relatively low first ionization energy (more information about propellant selection is given in section 3.4).

For a peak field strength of 30mT and an approximate electron temperature of 30eV,  $r_e = 1.042$  mm and  $r_i = 1142.079$  mm for krypton. Diagrams showing the geometry and significant dimensions of the thruster are shown in Fig. 2 and photos of the assembled thruster are shown in Fig. 3.



(a) Quarter-section view of thruster assembly. (b) Cross-section with significant dimensions (mm) shown.

**Fig. 2:** CAD diagrams of the thruster assembly with electromagnets omitted. Subfigure (a) shows a quarter-section view and subfigure (b) shows a cross-section view with significant dimensions labeled.

---

<sup>1</sup>Electron temperature may be estimated as a fraction of the operating voltage with units of eV. Goebel and Katz [4] cite Haas [14] in declaring that  $T_e \approx V_b/10$  in magnitude. The authors used Haas' estimate, but note that very recent Thomson scattering measurements, such as those taken by Dubois and Tsikata [15] in 2022, place this figure at closer to  $T_e \approx V_b/5$ .

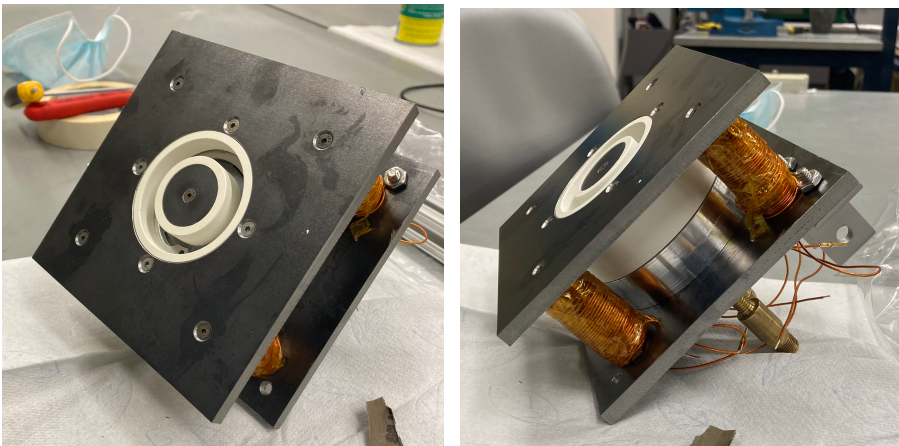


**Fig. 3:** Photos of the assembled thruster with electromagnets exposed. During testing, an aluminum shield (visible in Fig. 10) was wrapped around the thruster between the shunt plates to shield the internals.

Two methods may easily be used to generate the necessary magnetic field: electromagnets and permanent magnets. Permanent magnets have the advantage of being reliable, functioning independently of a power source, and operating without generating excess heat, but are limited by field strength, Curie temperature, and cannot be varied. Electromagnets produce a variable magnetic field limited only by available power supply and current-carrying wire heat rating. In either case it is necessary to use a magnetic shunt to direct the field into the necessary shape. Shunts operate on the principle of ferromagnetism; when a piece of ferromagnetic material is subjected to a magnetic field, the material behaves as a collection of smaller, connected magnets. As such, magnetic fields tend to be “conducted” by shunts, forming a “magnetic circuit” of field loops. A CAD model of the magnetic shunt used in development of this thruster is shown in Fig. 4

Ideally, the magnetic field should be as strong as possible (limited by the size of physical magnets, the extreme heating of electromagnets, and the gyro-radius of your ionized propellant). In order to generate the required radial field shape the shunt was designed to have one pole at the outer wall of the channel and one pole at the inner wall, so that the magnetic field lines orient themselves from one pole to another across the channel. Estimating the channel exit-plane field strength becomes difficult with a shunt because magnetic fields traveling through a shunt are weakened and may produce complex field geometries. As such, the modeling software COMSOL Multiphysics was used to iteratively design the shunt to produce the desired magnetic field shape and the field strength in the channel was verified directly with a Gauss meter after assembly. The COMSOL model of the magnetic field geometry generated by the shunt, along with theoretical and experimental measurements of field strength may be seen in Fig. 5. To summarize the magnitudes of the electric

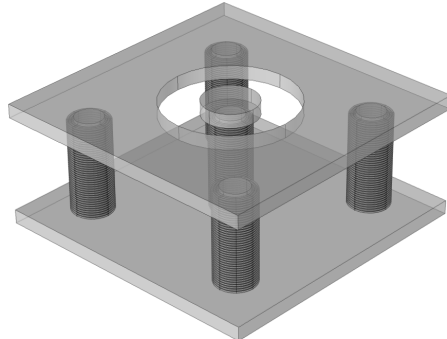


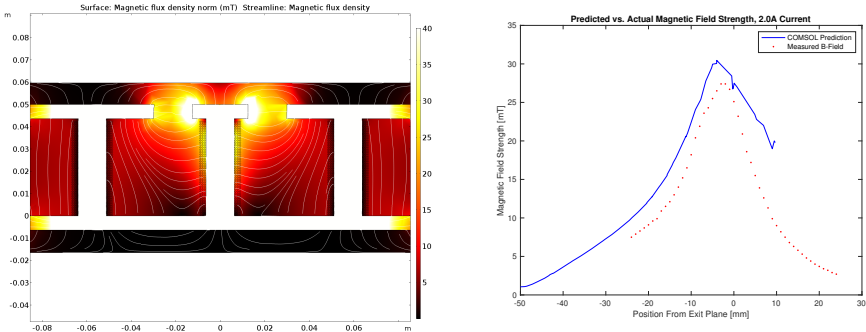
**Fig. 4:** CAD model of the thruster electromagnets and shunt. The shunt consists of a top and bottom plate connected by five rods that double as electromagnet cores. The magnetic field is generated by one inner and four outer electromagnets; the inner electromagnet is polarized opposite the outer electromagnets to generate magnetic field loops that cross the channel radially.

and magnetic fields within the thruster: the magnetic field peaks at a strength of 30mT near the exit plane of the channel and the anode potential is 300V. The anode used in the thruster consists of a flat steel ring placed atop the gas injector and it has holes to allow propellant to flow into the channel. This anode ring is held in place by a steel retaining ring that is set into the walls of the channel. A cross section of this stackup is shown in Fig. 2 and is visible in the left photo in Fig. 3.

### 3.4 Propellant Selection and Channel Length

Selecting a propellant requires balancing ease of ionization, mass, and cost of acquisition. Xenon is a conventional propellant because of its low ionization energy and high particle mass, but it was prohibitively expensive for this project. Krypton is the next largest noble gas and thus has a distinctly higher ionization energy than xenon; however it was selected as the propellant because it fit the project's budget. Consequences of this choice are twofold: first, a stable plasma of krypton requires a higher electron temperature since higher-energy collisions are required to free electrons from neutral atoms. Secondly, krypton is lighter than xenon so it produces less thrust for an identical volumetric flow rate. Hence, more krypton propellant would need to be stored aboard a spacecraft than a xenon-propelled counterpart.

Neutral propellant is dispensed out of a diffuser at the bottom of the channel. As neutrals diffuse through the channel, they make contact with the cloud of trapped high-energy electrons in the ionization region. The ionizing mean free path through the channel is the average distance a neutral propellant atom will travel before experiencing an ionizing collision with an electron. Maximizing the amount of propellant ionized maximizes thruster efficiency, dictating



(a) Cross-channel B-field lines (colorbar in mT). (b) Predicted and measured B-field strength.

**Fig. 5:** COMSOL Multiphysics models of (a) magnetic field shape and (b) strength and experimental measurements of field strength as a function of depth. The field was designed to peak at the exit plane at a strength of 30mT. The measurements in (b) were made in the center of the thruster channel (halfway between the inner and outer walls) and position 0 corresponds to the exit plane of the channel.

a channel length which should be significantly longer than the ionizing mean free path, but not so long as to cause losses in performance due to interactions with a larger surface area (allows electrons to lose energy via collision). Generally, this length is chosen to be of the same order of magnitude as the mean free path length,  $\lambda$ . A method of calculating  $\lambda$  is given by Goebel and Katz [4] as

$$\lambda = \frac{v_n}{n_e \langle \sigma_i v_e \rangle} \quad (12)$$

where  $v_n$  is the axial velocity of a neutral propellant atom,  $n_e$  is the channel electron number density, and  $\langle \sigma_i v_e \rangle$  represents the ionization "cross section" (which quantifies the probability of ionization) of the neutral propellant for collisions with electrons at a particular electron temperature. The quantity  $v_n$  can be calculated using Bernoulli's equation, given the parameters of a particular feed pipe system and propellant flow properties. To further reduce the  $v_n$  term (and thus the overall mean free path), the team designed a gas diffuser which ejects propellant azimuthally (a full description is given in section 3.5).

The ionization cross section,  $\langle \sigma_i v_e \rangle$ , is an experimentally derived value that varies with propellant type and electron energy level. To determine  $\langle \sigma_i v_e \rangle$  for krypton at 30eV electron temperature, the authors used first ionization cross section data reported by Loch et al. [16] with help from the web tool Web-PlotDigitizer<sup>2</sup> to extract graphical data. The LXCat<sup>3</sup> plasma data exchange

<sup>2</sup><https://automeris.io/WebPlotDigitizer/>

<sup>3</sup><https://nl.lxcat.net/home/>

project may also be a useful resource for readers seeking ionization data for a wide variety of propellants.

The number density of electrons,  $n_e$ , is more difficult to determine. During the design process an estimated value for  $n_e$  was selected that resulted in a calculated mean free path of 1.955–1.976 mm which was used to design the thruster channel. Much later on, however, the estimate for  $n_e$  was determined to be incorrect, and so this mean free path estimate could not be used to validate the length of the channel.

A process is described by Goebel and Katz [4] for choosing a channel length based on the axial ionization region length,  $L$ . This length represents the depth of the plasma within the channel and hence the region within which neutral ionization is most likely to occur.  $L$  may be calculated as

$$L = \frac{4\pi T R e v_n w}{M \langle \sigma_i v_e \rangle}. \quad (13)$$

where  $T$  is thrust,  $R$  is the channel outer diameter,  $w$  is the channel width, and  $M$  is the mass of a propellant atom. The ratio between  $L$  and the mean free path  $\lambda$  determines the percentage of neutrals that leave the thruster ionized; to increase ionization efficiency,  $L > \lambda$ . Goebel and Katz further report that the relationship between plasma length and fraction of ionized neutrals is

$$L = -\lambda \ln(1 - p) \quad (14)$$

where  $p$  is the decimal fraction of neutrals that leave the thruster ionized. Once both  $\lambda$  and  $L$  have been set, the channel length is to be the sum of the length  $L$  and the length required for the magnetic field to approach zero at the anode (Goebel and Katz report that the magnetic field gradient increases thruster performance).

With the aforementioned estimate for mean free path, 99% ionization ( $p = 0.99$ ) yields a target ionization region length of 9.00 mm, per equation 14. Given the simple design of this thruster's magnetic shunt (the resultant fields of which are visible in Fig. 5b), it was not practical to create a channel so deep that the radial magnetic field reached a magnitude of near zero. The team ultimately selected a channel length of 10 mm which is reflected in the final thruster design as the vertical distance from the exit plane to the top of the exit ring.<sup>4</sup> Although this channel length was not sufficiently long to allow the magnetic field gradient to fall to zero, it met the required physics criteria:  $L = 10$  mm exceeds the 99% neutral ionization region length of 9.00 mm;  $L \gg r_e$  to assure electron trapping; and  $L \ll r_i$  to allow ion escape. During a design review with subject matter experts, a channel length on the order of 10 mm was considered reasonable, and even slightly long; however, as mentioned

---

<sup>4</sup>It may be noted that the channel depth shown in Fig. 2 (b) marks 12 mm as the distance between the anode plate and the exit plane; a 2 mm thick stainless steel retaining ring which holds the anode plate in place extends above the bottom-most part of the channel. This ring is also at anode potential, yielding an ring-to-exit plane distance of 10 mm.

earlier, it was eventually determined that the estimated value for  $n_e$  which was used to generate the mean free path estimate was incorrect.

### 3.5 Propellant Diffuser

In this thruster the propellant diffuser serves to deliver gaseous propellant to the thruster channel and to electrically isolate the anode plate from the gas feed pipes. Propellant delivery has two primary considerations: even distribution, and propellant longevity. It is advantageous for propellant to remain within the channel for as long as possible (longevity) because this increases the amount of time in which propellant neutrals may experience an ionization event. Axial injection of propellant reduces longevity by providing a straight-line path for propellant to exit the channel, so to create a longer path and introduce turbulence into the gas flow, the team designed a diffuser which injects propellant azimuthally. This was achieved by flowing the propellant into the diffuser through two inlet holes which filled a toroidal plenum that served to more evenly distribute the pressure profile radially. Branching off of this toroidal plenum were a number of helical channels which carried the propellant to the channel. These helical tubes redirected the propellant's trajectory such that it was injected into the channel with an azimuthal trajectory. The concept of azimuthal propellant injection has previously been explored in a limited context, with a previous study reporting higher performance of a cylindrical HET with azimuthal injection than radial injection [17], but the method of injecting propellant via a plenum and series of tubes all entirely composed of cavities within a unibody component is unique among diffusers. Furthermore, the particular geometries used in the final design of this diffuser cannot be fabricated with subtractive manufacturing techniques, so must be 3D printed. For these reasons the team filed a patent for the part.

Three types of manufacturing were pursued for various iterations of the diffuser: stereolithographic resin (SLA) printing, direct metal laser sintering (DMLS) printing, and ceramic sintering. SLA manufacturing was successfully performed using Somos PerFORM, which is a high temperature SLA resin that has previously been used in 3D printed cold gas thrusters [18]. DMLS manufacturing was successfully performed using an aluminum alloy and followed by sulfuric anodization to MIL-A-8625F spec in order to create an electrically insulative coating (allowing the aluminum component to serve as an electrical standoff). Ceramic sintering was attempted using Formlabs Ceramic Resin, which consists of silica particles suspended in a photopolymer resin. The component is first printed via SLA and then is fired in a kiln to burn out the resin and sinter the silica particles into a solid part. SLA printing failed due to the resin clogging a critical dispenser valve and so the ceramic part could not be completed.

As a material, the ceramic resin had both the thickest component wall-size requirement and was the most prone to clogs in the part cavities. These factors drove the low number and large diameter of the helical channels; future iterations of the diffuser may feature a greater number of distribution channels

with narrower diameters. A CAD model of the diffuser is shown in Fig. 6 and a photograph of three material prototypes is shown in Fig. 7. In addition to the aforementioned functional features, the diffuser included a carved-out channel at the outer edge of the component to allow passage for a wire used to set the anode plate voltage (this channel is visible only in the left-most diffuser in Fig. 7 because the outer diameters of the center and right-hand diffusers were shrunk to accommodate the anode wire). The anode plate rested on top of the diffuser and was held in place by a retaining ring inset into the channel walls.

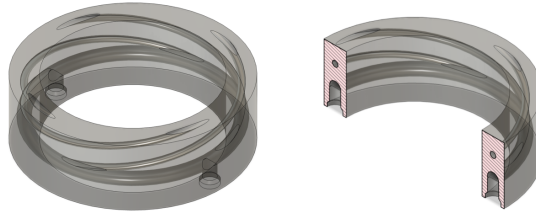


**Fig. 6:** Transparent CAD model and section view of the prototyped diffuser.



**Fig. 7:** Photograph of three diffuser prototypes. Left: low-temperature SLA resin used to prototype the dimensions for the ceramic diffuser. Center: high-temperature SLA resin prototype (Somos PerFORM) used in the tested thruster configuration. Right: aluminum DMLS prototype with black anodized coating to ensure electrical insulation.

### 3.6 Cathode Design

To avoid the engineering complexities associated with hollow cathodes, the team developed a Wehnelt cylinder to act as an electron source for ignition (the thrust plume would be neutralized by grounding the chamber walls). For their simplicity and ability to "focus" a beam of electrons, Wehnelt cylinders find common use in scanning electron microscopes [19]. Operating on the principle of high-temperature thermionic emission, the cathode consisted of a V-shaped, 0.13mm pure tungsten filament placed within a cylindrical cavity

16 *Undergraduate Hall Thruster*

in a copper case with a single exit hole (this case serves the role of a Wehnelt cap). For thermal considerations, the case was manufactured out of copper with a thermally applied black-oxide surface to increase emissivity. The case was electrically biased negative relative to the filament by means of a resistor in order to direct the beam of electrons out of the cavity. Applying a high current to the filament causes the temperature to rise and, when the work function of tungsten is exceeded, causes electrons to be thermionically emitted. New electrons from the power supply refill the filament to replace those lost (also preventing emitted electrons from being pulled back to the filament by setting up a local electric field at the tip of the V). The cylinder fills up with negative charges and the negative bias on the case causes electrons to be expelled from the cylinder through the hole in the case. Once outside the case, the electrons are drawn into the thruster channel due to the high anode potential. CAD models of the cathode assembly are shown in Fig. 8. A cathode circuit is shown in Fig. 9, along with a simulation of filament emission made from provided data (Goebel, D., personal communication, Oct 15, 2021). Experimental lifetime testing of the cathode revealed a current of 2.5A to be the highest sustainable current that did not cause the filament to rapidly burn out. This 2.5A filament current corresponds to a theoretical emissive current of 41mA. During operation, however, the anode within the channel read a peak current of around 9mA, indicating significant losses of electrons along the path from the cathode to the anode.

Although this emissive current falls well below the 1A electron current necessary to neutralize the thrust plume, experts in the field indicated that thruster ignition is possible with thermionic filaments held very close to the thruster channel, with the plume being neutralized by grounded test chamber walls.

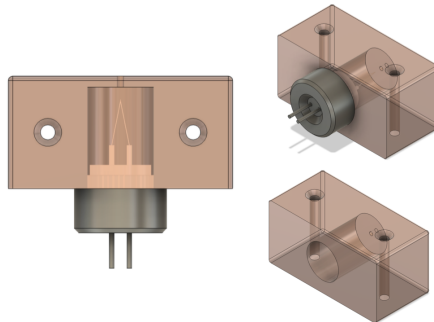


**Fig. 8:** Various views of a CAD model of the Wehnelt cylinder assembly. The case is made from copper and the filament is attached to a modified aluminum Hitachi S-type filament cartridge mount used in a scanning electron microscope.

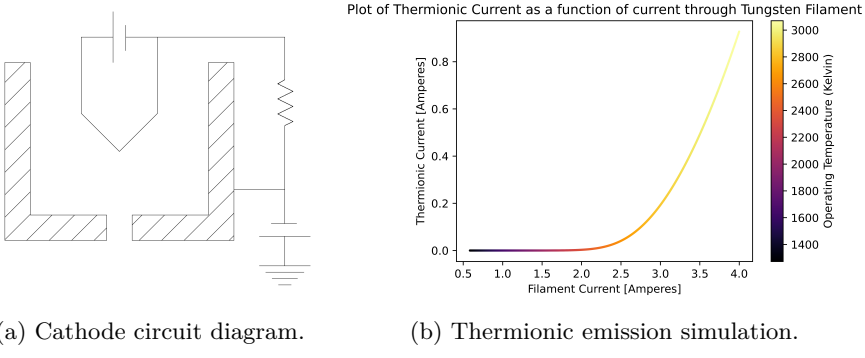


**Fig. 9:** Cathode diagrams. Subfigure (a) shows a circuit diagram for the cathode and subfigure (b) shows a graph of thermionic-emission current as a function of current passed through a 0.13mm pure tungsten filament. It should be noted that although the melting point of tungsten is 3,695 K, the filament consistently demonstrated failure at lower temperatures.

## 4 Low-Cost Thrust Stand Design

To measure the small output thrust that is produced by most HETs, it is necessary to introduce a combination of a) rigid sensing structures with high precision strain gauges or balances and b) force multiplying apparatuses to increase the signal range for the sensor to interpret. Because of the high cost associated with high precision gauges and balances, this team chose to incorporated methods of mechanical and electrical signal amplification to achieve force measurement sensitivities at the millinewton level.

### 4.1 Mechanical Design

The thrust stand incorporates a hanging lever arm and stand to multiply output force with minimal gravitational influence. This system has two main components: an upright structure and a pendulum/lever arm. The main structure consists of two upright trusses attached by horizontal framing. This structure supports a vertically hanging pendulum and contains a mount for a piezoelectric force sensor. At the top of each truss is a piece of sheet metal with a concave u-shaped notch cut into it. The pendulum arm is firmly clamped at one end to the center of a perpendicular iron rod, which acts as the pendulum axle. The ends of this rod rest in the sheet metal notches, which constrain the horizontal and vertical motion of the arm and minimize contact area, to act like a low friction bearing. The HET is mounted to the other end of the lever arm, oriented tangent to the axis of rotation. An annotated photograph of the thrust stand is shown in Fig. 10.

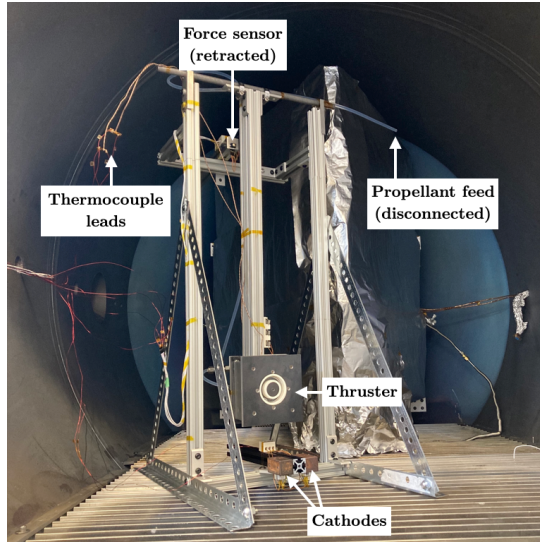


**Fig. 10:** Annotated photograph of the thrust stand setup inside the MIT SPL AstroVac test chamber. The force sensor is located at the end of an arm which is extended to contact the pendulum arm at equilibrium; the arm is retracted in this image.

The arm is allowed to fall freely to an equilibrium position and then a piezoelectric force sensor attached to the end of a rigid bar is extended to contact the arm near the top, just below the axle (on the side of the pendulum opposite the thruster). This setup causes the pendulum to act as a lever arm, allowing the sensor to measure a higher force than is exerted by the HET. The gain is set by the relative distances between the force sensor, HET, and pivot. Importantly, this arrangement of the sensor causes the pendulum arm to remain static under load (i.e. the pendulum never rotates), eliminating the need to account for dynamic friction forces. Frictional and other losses (such as torque from the propellant feed pipes) are accounted for all at once with a calibration curve in which a known force is applied at the thruster's point of contact and the force response is measured by the piezoelectric sensor. The team performed this calibration by applying an arbitrary force curve to the center point of the HET using a matched force sensor and compared the applied and measured load curves. This calibration scheme directly characterizes lever arm gain and losses all at once, eliminating the need to estimate losses.

## 4.2 Instrumentation

The thrust stand includes harnessing for two types of measurement: temperature and force. Force measurements were taken with a Honeywell FSG005WNPB, a piezoresistive sensor with an internal Wheatstone bridge.

Temperature measurements were taken with Digilent 1286-1099-ND, type-K thermocouples. One was placed near the bottom of the channel, contacting the diffuser, and the other was attached to the central electromagnet of the thruster. These locations were motivated by a concern for overheating the central electromagnet (where heat transport would be most difficult) and a desire to track the temperature of the PerFORM diffuser during firing. Both thermocouple wiring harnesses ran along the arm of the thrust stand and were attached to the fulcrum to reduce torques or other loads on the arm (this was similarly done with the propellant feed tubes). All signal wires were passed through an instrumentation feedthrough out of the vacuum chamber and were amplified air-side. The thermocouple signals were amplified using Maxim MAX31855 thermocouple amplifiers and the force sensor measurements were amplified with an Analog Discovery AD623AN instrumentation amplifier. An Arduino script converted the output of the amplifier boards into temperature readings in Celsius and force measurements in millinewtons. The central electromagnet temperature data was used for real-time monitoring and throttling of the electromagnet circuit current to avoid nearing the temperature threshold of the Kapton tape. The diffuser temperature data was intended to be recorded so that damage to the PerFORM diffuser (observed after testing) could be correlated to the maximum temperature reached by the resin, thus informing whether PerFORM is a viable material for use in future HETs. For reference, PerFORM reportedly has a deflection temperature of 268°C with a post-cure, but the burning temperature is not reported (though is presumably much higher than the deflection temperature).

The expected thrust was on the order of 30 mN. The Honeywell sensor was used at an operating voltage of 5V, resulting in a sensitivity of 33.7612 mV/N. The Arduino Uno contains an internal 10-bit analog to digital converter (ADC) that returns signals in the range 0-5V as integer steps in the range 0-1023, corresponding to approximately 1 step per 5 mV, hence significant amplification was required to measure forces on the order of 30 mN. The force sensor was mounted at a distance above the thruster so as to result in a lever gain of 7.33 without any electronics. The Maxim instrumentation amplifiers were set to a gain of 31.84 (using 3.24 kΩ resistors). Together, the voltage passed to the Arduino corresponded to 1614 ADC steps per Newton of thrust, corresponding to a measurement range of 0 to 0.62 N at a resolution of approximately 3 ADC steps per 2 mN of thruster force. This is relatively low precision, but would suffice to validate the order of magnitude of thrust produced.

### 4.3 System Integration & Vacuum Considerations

The complexity of system integration depends heavily on the chamber, sensing suite, and associated components. For many systems, however, the main trade offs will be between reliability and vacuum operation. Depending on the chamber in use, to pull ultra-high vacuum one should minimize outgassing by using vacuum compliant materials. For the system used in this project, the

main integration challenges fell into the following categories:

**Gas Flow** – Flow rate was controlled with two Omega FMA6502ST display-less gas controllers, though issues in the feed lines and control software called into question the reliability of the devices. All pipe/tube connections were made with 1/4” Swagelok fittings. Generally, testing gas lines for leaks using indicator solution (or another method) is recommended prior to testing.

**Wiring Harness** – The main harnessing challenge was establishing reliable continuity between air and vacuum side components through the wall of the vacuum chamber. Necessary lines included signal wires for the thermocouples and force sensor; power wires for the cathodes and electromagnets; and external power supply grounding connections (though a separate high-voltage connection was used to pass the anode voltage). A harness was constructed to pass lines through a MIL-C-26482 19-pin Conflat-style flange. The high-voltage anode and high-current magnet lines were run with 20 AWG Kapton-insulated wire and 22 AWG enameled magnet wire was used to run the signal and cathode lines; both types of insulation are known to be low-offgassing. Generally it was found that ceramic terminal blocks served as effective intermediaries between harnessing and thruster/cathode wires. Each harness line consisted of a wire that on one side had a female vacuum-safe crimp connector that was crimped, soldered, and insulated in Kapton tape, and on the other was stripped bare. Bare sides generally fed into one end of a terminal block while wires extending out of the back of the cathode and thruster fed into the other end. Fig. 11 shows a block diagram of the connections made with the wiring harness.

**Offgassing** – Vacuum tradeoffs are often made between reliability and vacuum materials. Generally, outgassing is a significant problem for chambers that have a small volume, a less capable pumping system, or which operate at higher vacuum levels. For these systems, minimizing the use of materials that release volatile organic compounds (VOCs) or other gasses keeps the chamber clean and allows high vacuum states to be more easily reached and maintained. For instance, Kapton is a commonly used material for its properties of electrical insulation and thermal conduction. A database of common materials and outgassing properties can be found online at [outgassing.nasa.gov](http://outgassing.nasa.gov) [20].

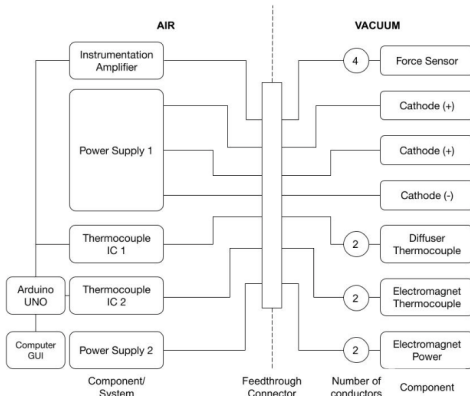


**Fig. 11:** Block diagram of connections made with the wiring harness.

## 5 Test Results

### 5.1 Testing at AstroVac

Testing was conducted at the MIT Space Propulsion Laboratory's AstroVac chamber. A high voltage line was supplied by MIT SPL and benchtop power supplies were used to power the cathode and electromagnet circuits and to drive all instruments. Data signals from instruments were interpreted by an Arduino Uno and passed to a laptop computer which logged the data and provided human-readable telemetry in real time. The AstroVac chamber contained two flow controllers<sup>5</sup> calibrated for volumetric flow of nitrogen, each with a maximum flow rate of 10 sccm. Nominal flow rate into this thruster was 20 sccm of krypton, which (with a scaling factor to convert from nitrogen to krypton flow rates) necessitated a programmed flow of 6.88 sccm per flow controller, with the streams rejoined prior to entering the thruster. Throughout the course of testing, various debugging activities took place including correcting the grounding condition of the high voltage power supply, bleeding air that was trapped in the gas distribution lines, and repairing a cathode which was initially dead on arrival. Despite a plethora of swept operating conditions, ignition was not achieved. A summary of the parameters and ranges swept during testing is shown in table 1. It is notable that the maximum current read by the anode power supply during testing was 9 mA, implying successful electron generation and transport into the thruster channel, though at significantly lower levels than were predicted by the electron emission model (assuming full transport of electrons into the channel).

---

<sup>5</sup>The authors note that the flow controllers were calibrated by a third party prior to testing, but throughout the testing process unexpected tank pressure fluctuations were observed in response to programming the flow controllers. These anomalies could not be thoroughly investigated by the team, so some doubt exists as to whether the correct propellant flow was successfully delivered to the thruster.

	Nominal	Min	Max	Min	Max
Propellant	Kr	Ar	Ar	Kr	Kr
Cathode 1 Current [A]	2.5	2.5	3.0	3.0	3.3
Cathode 2 Current [A]	0	0	3.0	3.0	3.3
Electromagnet Current [A]	3.0	4.0	4.0	4.0	5.12
Anode Voltage [V]	300	300	500	300	500
Flow Controller 1 [sccm]	6.88	4.8	7.0	7.0	10.0
Flow Controller 2 [sccm]	6.88	4.8	7.0	7.0	10.0

**Table 1:** Summary of parameters and ranges swept during testing.

## 5.2 Next Steps

Two theories for the failure to achieve ignition were provided by expert reviewers. The first theory is that a space-charge limit was reached in the main channel of the thruster. The cathodes used in this test were purely thermionic emitters, so only electrons were being supplied to the channel. It is possible that a contributing factor to why a much smaller anode current was measured than was being emitted by the cathodes was that the trapped electrons in the channel formed a negative space charge that prevented additional electrons from entering the channel. This would have resulted in a channel electron density below the necessary density to achieve and sustain ignition. The second theory is that not enough electron current was supplied to enable ignition, as previous thrusters have referenced cathode currents of a similar magnitude as the operating current of the thruster [21]. It was assumed in the development of this thruster that such high cathode currents were necessary only to neutralize the thrust plume (which the cathodes in this design were never intended to do; the thrust plume would be neutralized by the walls of the grounded chamber), so a total cathode emissive current of 82 mA fell far below the designed thruster discharge current of 1.125 A.

Both theories can be addressed at once by using a plasma-source cathode, such as a hollow cathode, rather than a thermionic emitter. Plasma-source cathodes are capable of producing high electron currents and supply both ions and electrons to the thruster environment. The electron current could serve both to aid ignition and to neutralize the thrust plume, while the ions provide an opportunity for a theorized electron space charge in the channel to be neutralized and thus allow a higher electron density to form inside the channel prior to ignition. As of the date of publication, a subset of the authors/original team members intend on pursuing cathode development in an independent study for the fall 2022 semester with the aim of developing a plasma source capable of igniting the thruster; ideally, this will involve no design changes to the thruster itself.

## 6 Conclusion

A multi-institutional team of undergraduate students designed and conducted an independent study program that simulated the research process and provided an opportunity to study, design, fabricate, and test a Hall effect thruster.

Although the thruster did not successfully ignite during testing, correspondence with subject experts revealed tangible next steps that point towards the development of a cathode/plasma source, rather than design flaws in the thruster itself. Meanwhile, the educational goals of the project were highly successful in that the team demonstrated that HETs can be utilized to teach research, physics, and engineering skills to undergraduate students through the medium of a self-directed project course. This was demonstrated by the delivery of a fully integrated HET and thrust stand and the performance of testing activities in a laboratory setting. Furthermore, the delivery of typical engineering research artifacts including literature review notes, written grant proposals, manufacturing diagrams, and technical documents (including a provisional patent and this publication) serve as evidence of the learning process. Regarding design, the completed device poses a significant iteration and variation on prior undergraduate thrusters [1, 3] driven by design calculations based on fundamental physics principles. A final point of success is that this project brought together physicists, astrophysicists, and engineers with varied academic backgrounds from Wellesley College, Olin College, and Brandeis University and created an environment in which the students were able to teach and learn from each other. They found common ground and have brought aerospace engineering to their home institutions while broadening their education through this multidisciplinary, hands-on application.

**Acknowledgments.** The authors thank Professor Paulo Lozano and graduate students Madeline Schroeder and Matthew Corrado for the donation of their time and laboratory resources to make testing possible. The team also thanks Dr. Dan Goebel, Dr. James Szabo, Dr. Manuel Martinez-Sanchez, Dr. Jonathan Walker, Kyle Emmi, Nathan Cantrell, and Lucas Ewing for serving as design review board members; Justin Kunimune for attending the design review and for creating Fig. 1; and Aissa Conde for contributing to design discussion meetings. Finally, the team thanks Dr. Ryan Conversano for answering questions during the learning phase of this study, Louis Perna for providing valuable insights into thrust stand design, Diane Covello for guiding the patent application process, and Matthew Neal for providing the Hitachi filament mounts used in the cathodes.

## Declarations

### Funding

This work was supported by funding from a Babson, Olin, Wellesley Three College Collaboration Presidential Innovation Grant and the Massachusetts Space Grant Consortium. Funding for attendance at IEPC was provided partially from the Presidential Innovation Grant and partially from an Olin College Student Activities Grant.

## Conflict of interest/Competing interests

Not applicable.

## Data availability

Not applicable.

## Code availability

Not applicable.

## Authors' contributions

All authors contributed to the conception, design, and execution of the study. Design, fabrication, and testing of the thruster was done by Braden Oh, Albert Countryman, Mahderekal Regassa, Avery Clowes, Grant Miner, and Marissa Klein. The test stand was designed and fabricated by S.C. "Mack" McAneney and Simon Kemp. The original draft of the manuscript was written by Braden Oh and Albert Countryman with contributions by the other authors. Braden Oh, Albert Countryman, and Christopher Lee made substantial contributions to edits and revisions for important technical content. Additional edits and revisions of the document were made by the other authors. All authors read and approved the final manuscript.

## References

- [1] Baird, M.: Designing an accessible hall effect thruster. In: Honors Theses. Western Michigan University, Kalamazoo, MI (2016)
- [2] Hopping, E.P., Huang, W., Xu, K.G.: Small hall effect thruster with 3d printed discharge channel: Design and thrust measurements. Aerospace **8**(8), 227 (2021)
- [3] Oh, B., Kunimune, J.H., Spicher, J., Anfenson, L., Christianson, R.: Undergraduate demonstration of a hall effect thruster: Self-directed learning in an advanced project context. In: 2020 ASEE Virtual Annual Conference Content Access. ASEE Conferences, Virtual On line (2020)
- [4] Goebel, D.M., Katz, I.: Fundamentals of Electric Propulsion: Ion and Hall Thrusters. NASA Jet Propulsion Laboratory, Pasadena (2008)
- [5] Conversano, R.W., Goebel, D.M., Hofer, R.R., Matlock, T.S., Wirz, R.E.: Development and initial testing of a magnetically shielded miniature hall thruster. IEEE Transactions on Plasma Science **43**(1), 103–117 (2014)
- [6] Conversano, R.W.: Low-power Magnetically Shielded Hall Thrusters. University of California, Los Angeles, Los Angeles (2015)

- [7] Warner, N.Z.: Theoretical and experimental investigation of hall thruster miniaturization. PhD thesis, Massachusetts Institute of Technology (2007)
- [8] Martinez-Sanchez, M. and Lozano, P., via MIT OpenCourseWare: 16.522 Space Propulsion Spring 2015 Lecture Notes. <https://ocw.mit.edu/courses/16-522-space-propulsion-spring-2015/pages/lecture-notes/> (2015)
- [9] Sankovic, J.M., Hamley, J.A., Haag, T.W.: Performance evaluation of the russian spt-100 thruster at nasa lerc. In: International Electric Propulsion Conference (1994)
- [10] Miller, R.K.: Lessons from the olin college experiment. Issues in Science and Technology **35**(2), 73–75 (2019)
- [11] Silverman, M.P.: Self-directed learning: a heretical experiment in teaching physics. American Journal of Physics **63**(6), 495–508 (1995)
- [12] Dannenmayer, K., Mazouffre, S.: Elementary scaling relations for hall effect thrusters. Journal of Propulsion and Power **27**(1), 236–245 (2011)
- [13] Lee, E., Kim, Y., Lee, H., Kim, H., Doh, G., Lee, D., Choe, W.: Scaling approach for sub-kilowatt hall-effect thrusters. Journal of Propulsion and Power **35**(6), 1073–1079 (2019)
- [14] Haas, J.M.: Low perturbation interrogation of the internal and near-field plasma structure of a hall thruster using a high -speed probe positioning system. PhD thesis, University of Michigan, Ann Arbor, MI (2001)
- [15] Dubois, T., Tsikata, S., Chung To Sang, M., Garrigues, L.: Insights into hall thruster radial physics via incoherent thomson scattering. In: International Electric Propulsion Conference (2022)
- [16] Loch, S., Pindzola, M., Ballance, C., Griffin, D., Mitnik, D., Badnell, N., O'Mullane, M., Summers, H., Whiteford, A.: Electron-impact ionization of all ionization stages of krypton. Physical Review A **66**(5), 052708 (2002)
- [17] Ding, Y., Jia, B., Xu, Y., Wei, L., Su, H., Li, P., Sun, H., Peng, W., Cao, Y., Yu, D.: Effect of vortex inlet mode on low-power cylindrical hall thruster. Physics of Plasmas **24**(8), 080703 (2017)
- [18] Gundamraj, A., Thatavarthi, R., Carter, C., Lightsey, E.G., Koenig, A., D'Amico, S.: Preliminary design of a distributed telescope cubesat formation for coronal observations. In: AIAA Scitech 2021 Forum, p. 0422 (2021)

26 *Undergraduate Hall Thruster*

- [19] Park, M.-J., Kim, D.H., Park, K., Jang, D.Y., Han, D.-C.: Design and fabrication of a scanning electron microscope using a finite element analysis for electron optical system. *Journal of mechanical science and technology* **22**(9), 1734–1746 (2008)
- [20] NASA Goddard Space Flight Center: Outgassing Data for Selecting Spacecraft Materials Online. <https://outgassing.nasa.gov/Home> (1993)
- [21] Katz, I., Hofer, R.R., Goebel, D.M.: Ion current in hall thrusters. *IEEE Transactions on plasma science* **36**(5), 2015–2024 (2008)